Tracing Be-star disk inclination, mass, and long-term evolution from Hα profiles in the entropy–complexity plane

A. Granada[1,2], A. R. Plastino[3], Y. R. Cochetti[4,5], T. A. A. Sigut[6], S. Charbonnel[7], O. Garde[7], P. Le Dû[7], L. Mulato[7], T. Petit[7], E. Bryssinck[8], R. Pomillo[9], and O. Thizy[10]

[1]CITECCA, Universidad Nacional de Río Negro, Argentina
[2]CONICET, Argentina
[3]UNNOBA & CONICET, Argentina
[4]Facultad de Ciencias Astronómicas y Geofísicas, UNLP, Argentina
[5]Instituto de Astrofísica de La Plata (IALP), CONICET–UNLP, Argentina
[6]Western University & Institute for Earth and Space Exploration (IESX), Canada
[7]2SPOT, France
[8]BRIXIIS Observatory, Belgium
[9]Promiod Observatory, Italy
[10]Observatoire de la Belle Etoile, France

E-mail: agranada@unrn.edu.ar

Abstract

The morphology of the Hα line in classical Be stars contains information on both the viewing geometry and the amount and distribution of circumstellar material. We summarize our recent use of the Shannon entropy H and the LMC statistical complexity C as compact descriptors of Hα line morphology. Synthetic profiles form well separated sequences in the entropy–complexity (H–C) plane: inclination primarily selects the sequence, while the disk mass drives the position along it. Observed late-type Be stars occupy the same regions of the diagram, supporting the use of the H–C plane as an inclination diagnostic.

Applied to the long-term spectroscopic record of β Psc, the same representation reveals a rapid excursion from the pre-event state toward a weak-emission, low-disk-mass state, followed by recovery and secular evolution. As an additional estimate presented here, we use the disk masses inferred from the Hα-sensitive model grid to quantify the strongest excursion. Within the adopted VDD model grid, the inferred disk mass decreases by about 0.7 dex, or a factor of ~ 5, and recovers essentially its pre-event value within ~ 370 days. If this recovery reflects genuine disk replenishment, the corresponding average net disk mass-growth rate is of order $4 \times 10^{-9}, M_{\odot}\,\mathrm{yr}^{-1}$. The recovery is also accompanied by a shift toward larger apparent inclinations in the H–C model grid, indicating that changes in disk geometry or line-emitting structure may contribute to the inferred mass evolution.

1 Introduction

Classical Be stars are rapidly rotating B-type stars surrounded by gaseous, nearly Keplerian circumstellar disks. Their Balmer emission lines, and Hα in particular, are among the most direct observational tracers of the disk. The line profile shape responds simultaneously to viewing angle, disk density structure, radial extent, and time-dependent disk evolution (Rivinius et al., 2013). Extracting physical information from morphology is therefore powerful, but it is also intrinsically degenerate when only a small set of conventional line observables is considered.

Information-theoretic quantities offer a complementary description in which the complete line shape is reduced to a small number of global descriptors. In recent work we mapped synthetic Hα

profiles of Be stars (Lailey & Sigut, 2023) onto the Shannon-entropy–statistical-complexity (H–C) plane (Granada et al., 2026a). The resulting diagram contains organized sequences rather than a featureless cloud: inclination largely separates the sequences, whereas disk properties control the displacement along them. The inclination ordering predicted by the models was subsequently tested with observed late-type Be stars (Granada et al., 2026b). An application to β Psc then showed that a time series in the same plane provides a compact representation of the star's long-term disk evolution (Granada et al., 2026c).

This contribution summarizes those results as presented at LIAC 42. The novelty of this manuscript is the **order-of-magnitude net disk mass-growth estimate** in Sect. 4.1, obtained by combining the observed H–C excursion of β Psc with the disk-mass calibration of the synthetic grid. Within the assumptions and parameter range of such a grid, the inferred mass is expected to be representative of the disk mass: substantial changes in the outer disk radius ($R_{\rm out}$), the density at the base of the disk (ρ_0), or the slope of the density distribution (n) that modify the disk mass also modify the Hα emission. The main uncertainties therefore arise from the adopted disk geometry and density prescription, and from interpolation within the finite grid.

2 From Hα line profiles to the entropy–complexity plane

We use the synthetic Hα library of Lailey & Sigut (2023), computed for an axisymmetric Be-star disk with density law

$$\rho(R,z) = \rho_0 \left(\frac{R}{R_*}\right)^{-n} \exp\left[-\left(\frac{z}{H(R)}\right)^2\right]. \tag{1}$$

For the subset explored in Granada et al. (2026a), the central star has $M_* = 4\,M_\odot$, $R_* = 3.5\,R_\odot$, $T_{\rm eff} = 13\,400$ K, and $\log g = 4.0$. The grid samples base density, radial density exponent, outer radius, and inclination. The original 11,550 profiles are reduced to 8,547 physically relevant cases by retaining, for each model family, only those outer radii for which increasing the disk radius still changes the Hα equivalent width by at least 1%. Thus, throughout the retained domain, changes in $R_{\rm out}$, ρ_0, or n that modify the integrated disk mass also leave a measurable imprint on Hα. We therefore use the integrated model mass, $M_{\rm disk}$, as an estimate of the disk mass within the assumptions of the grid.

Each continuum-normalized profile is transformed into a probability density by subtracting the continuum, rescaling the wavelength coordinate to $x \in [-1, 1]$, taking the absolute line excursion, and normalizing the area to unity. We then compute the Shannon entropy

$$H[p] = -\int p(x) \ln p(x)\, dx \tag{2}$$

and the continuous LMC structure indicator

$$C[p] = \exp(H[p])\, D[p], \qquad D[p] = \int p(x)^2\, dx, \tag{3}$$

following Catalán et al. (2002). In practice, the pair (H, C) provides a compact description of line spreading and structured departure from uniformity. The analysis presented here uses a spectral resolution $R = 10^4$ and focuses primarily on strong-emission profiles, for which the spherical treatment of the central star has the smallest impact on the diagnostic.

3 Inclination and disk mass in the model grid

The synthetic profiles form a family of arcs in the H–C plane. Different inclinations occupy different arcs, while disk parameters move models along a given arc. Figure 1 shows the strong-emission models colour-coded by their integrated disk mass. At fixed inclination there is a clear and monotonic ordering: higher H corresponds to lower disk mass, whereas the low-entropy end contains the

most massive disks (Granada et al., 2026a). This ordering is particularly useful, indicating that different combinations of ρ_0, n, and disk radius can generate broadly similar line strengths.

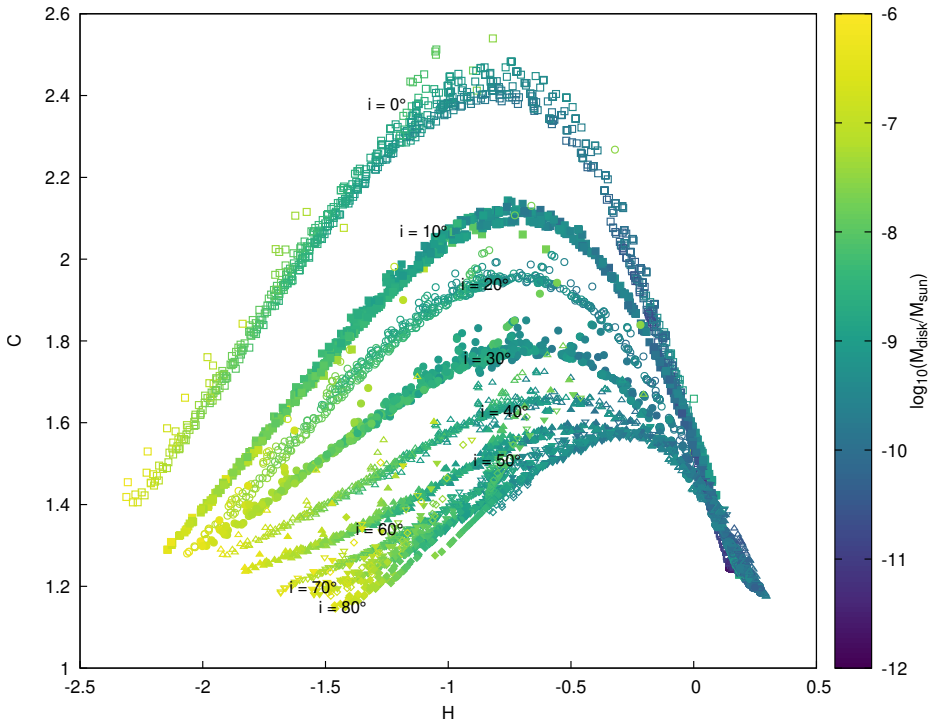


Figure 1: Strong-emission synthetic Hα models in the entropy–complexity plane. Symbols identify viewing inclination and colour gives the integrated disk mass, $M_{\rm disk}$, within the Hα-sensitive domain of the grid. As described by Granada et al. (2026a), inclination separates the main sequences, while disk mass orders the models along them.

The geometric interpretation can be tested with observed late-type Be stars. When the observed profiles are transformed in exactly the same way as the models, their locations fall in the same part of the diagram and follow the inclination ordering expected from the synthetic grid. This comparison is shown in Fig. 2. The result is encouraging because the diagram uses only the global morphology of one line, without fitting individual peaks, equivalent width, or a full radiative-transfer model to each observation. It therefore provides a rapid first estimate of disk orientation that can complement more detailed spectroscopic or interferometric methods.

The dependence of this mapping on inclination was explored explicitly by Granada et al. (2026c) (see their Appendix A). Separate $C_i(H)$ sequences and $\log M_{{\rm disk},i}(C)$ relations were constructed for different inclinations within the region of the model grid occupied by β Psc. The observational uncertainties in (H) and (C) were then propagated through the full interpolation procedure by Monte Carlo sampling, yielding corresponding distributions of inferred inclination and disk mass. Thus, the quoted disk-mass estimates account for the inclination dependence of the adopted H–C calibration and for the observational uncertainties entering the interpolation. They should nevertheless be regarded as model-dependent estimates: this procedure does not constitute a full exploration of the degeneracies that would arise from direct Hα-profile fitting with (ρ_0), (n), ($R_{\rm out}$), inclination, and other disk parameters varied simultaneously.

4 The long-term trajectory of β Psc

The H–C representation becomes especially informative when applied to a time series. For β Psc, the long-term Hα spectroscopic time series was assembled largely from spectra available in the Be Star Spectra (BeSS) database (Neiner et al., 2011). The observations trace a coherent path in the

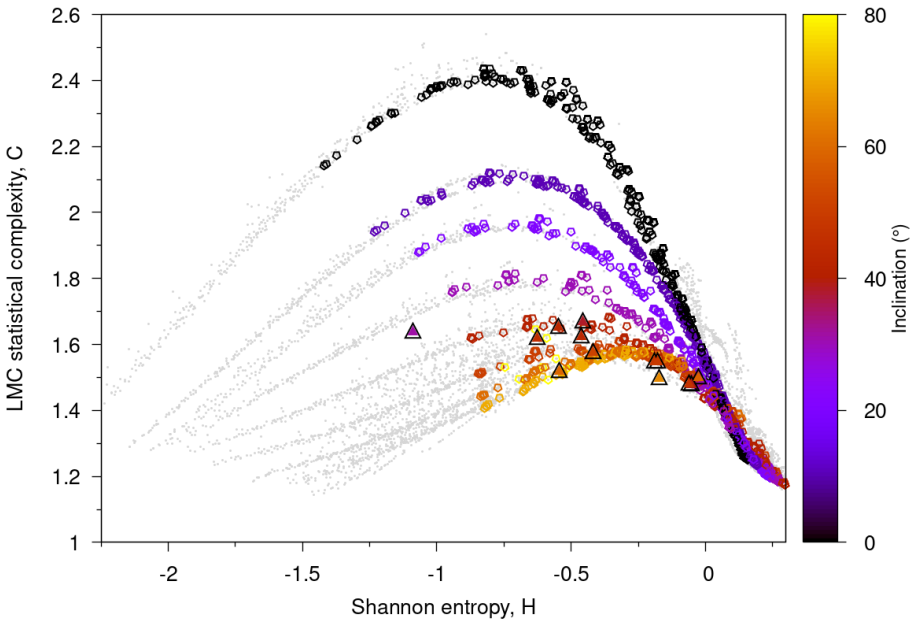


Figure 2: **Synthetic and observed late-type Be-star Hα profiles in the entropy–complexity plane. Grey symbols show the full synthetic model grid, while coloured penthagons indicate representative strong-emission models and large coloured triangles correspond to the observed stars HD 23552, HD 23630, HD 37795, HD 47054, HD 58715, HD 135734, HD 175869, HD 183914, HD 185037, HD 192044, HD 193911, HD 210129, and HD 217891. Some observed stars occupy nearly identical locations in the H–C plane and their symbols therefore overlap. Colours encode the disk inclination, using the values derived from detailed Hα profile modelling by Lailey & Sigut (2023) for the observed stars. As shown by Granada et al. (2026b), the observations populate the model-predicted regions and broadly follow the same inclination sequence.**

H–C plane rather than random epoch-to-epoch scatter.

Five representative states, labelled A–E in Fig. 3, summarize the main phases. The trajectory includes a rapid displacement from the pre-transition state, a low-complexity phase, a recovery, and slower secular evolution. By late 2025 the star had returned to a region close to its pre-transition location, while the most recent spectra indicated the beginning of a renewed displacement toward the transition region (Granada et al., 2026c).

This behaviour is consistent with the long-standing evidence that the Hα emission of β Psc evolves on multiple time-scales. Earlier detailed modelling found changes in disk radius and density over decades and showed that episodes of disk feeding can occur on much shorter, month-scale intervals (Levenhagen et al., 2021). The H–C trajectory does not replace such modelling; its advantage is that it exposes the sequence of morphological states in a compact, model-comparable plane.

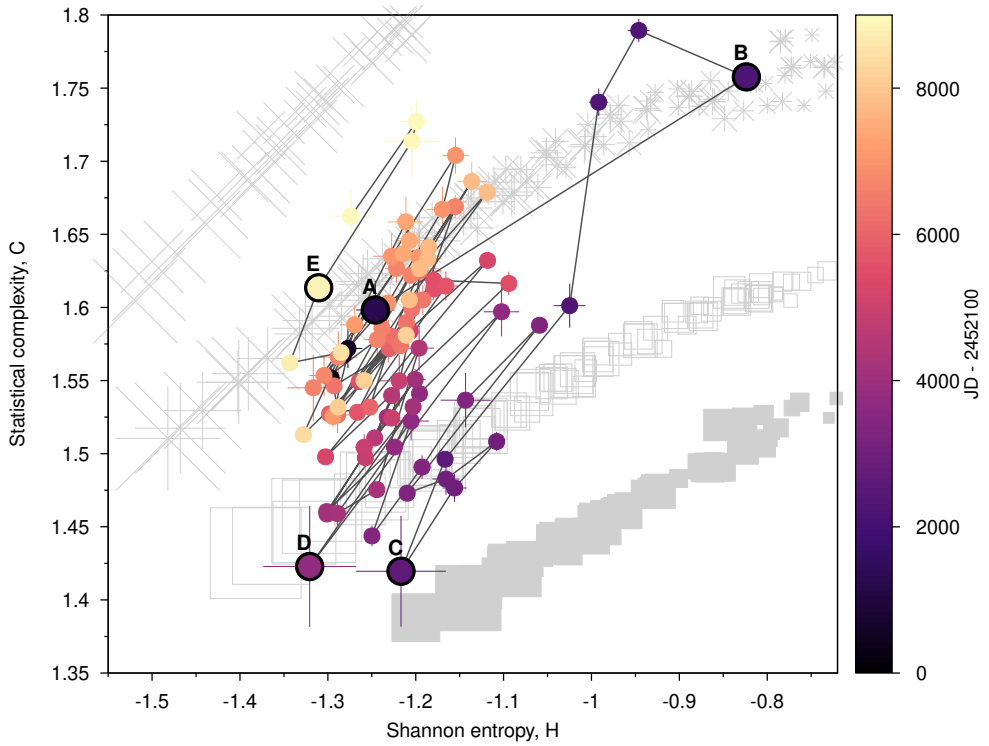


Figure 3: Long-term trajectory of β Psc in the entropy–complexity plane. Coloured circles represent observations, the colour scale gives time, and grey symbols show synthetic models. States A–E mark representative stages of the cycle (Granada et al., 2026c). The return of E toward A indicates a recovery of a line morphology close to the pre-transition state.

4.1 An order-of-magnitude net disk mass-growth estimate during the recovery

Over most of the time span covered by our Hα observations, the inferred disk mass remains confined within a relatively well-defined range. A remarkable exception occurs around $JD - 2452100 \simeq 2200$, when the inferred mass reaches $\log(M_{\rm disk}/M_\odot) \simeq -9.01$, about 0.7 dex below its pre-event value of $\simeq -8.30$ (see Granada et al., 2026c, for a detailed description of the disk parameter evolution). Within the adopted VDD model grid, this corresponds to a decrease in disk mass by a factor of ~ 5.

The inferred disk mass subsequently returns essentially to its pre-event level, from $M_{\rm disk} \simeq 9.8 \times 10^{-10}\,M_\odot$ at the minimum to $\simeq 5.0 \times 10^{-9}\,M_\odot$ about 370 days later. The implied increase is therefore $\Delta M_{\rm disk} \simeq 4.1 \times 10^{-9}\,M_\odot$. If this recovery reflects a genuine increase in disk mass rather

than a purely geometrical effect, it corresponds to an **average net disk mass-growth rate**

$$\dot{M}_{\rm disk,net} \simeq \frac{\Delta M_{\rm disk}}{\Delta t} \simeq 4 \times 10^{-9}\, M_\odot\, {\rm yr}^{-1}. \quad (4)$$

As an order-of-magnitude consistency check, the inferred **net change in disk mass** can also be related to the angular-momentum loss rate expected in a viscous decretion disk. If $\dot{M}_{\rm disk,net}$ is used as a characteristic scale for the stellar feeding rate, the stellar parameters adopted in our model grid, with an injection radius close to the stellar surface ($R_{\rm inj} \simeq 1.02 R_{\rm eq}$), give $|\dot{J}_*| \sim 3 \times 10^{34}\,{\rm g\,cm^2\,s^{-2}}$. This value lies within the 3×10^{34}–$5\times10^{35}\,{\rm g\,cm^2\,s^{-2}}$ range inferred for late-type Be stars (Ghoreyshi et al., 2023).

It is worth noting that this interpretation is not unique. During the recovery, the preferred location within the H–C model grid shifts from apparent inclinations of roughly 26°–30° near the minimum toward values around 40° when the inferred disk mass has recovered (Granada et al., 2026c). This shift may reflect changes in the structure or geometry of the Hα-forming region rather than a genuine reorientation of the entire disk. A tilt or warp of the outer disk remains one possible interpretation, but it is not uniquely required by the H–C diagnostic. The mass-growth estimate should therefore be regarded as an order-of-magnitude net change in the inferred disk mass, rather than as a direct measurement of the stellar mass-injection rate.

For comparison, viscous decretion-disk analyses of Galactic Be stars find mass-decretion rates spanning approximately 10^{-12}–$10^{-9}\,M_\odot\,{\rm yr}^{-1}$ (Vieira et al., 2017). These rates are not directly equivalent to the net disk mass-growth estimate derived here, because the latter measures the net change of the inferred disk mass over the observed recovery interval and may also contain a geometrical contribution. Moreover, the numerical value is based on interpolation within a grid computed for a representative late-type Be star, rather than on a dedicated time-dependent fit to β Psc; it therefore depends on the inclination track and on the finite sampling of disk density laws.

5 Conclusions

The entropy–complexity plane provides a simple representation of Be-star Hα morphology with a direct physical organization. In the synthetic grid, inclination separates the principal sequences and the integrated disk mass orders models along each sequence. Observed late-type Be stars populate the predicted regions, supporting the use of the diagram as a **rapid diagnostic of disk orientation within the domain of the adopted models**. For β Psc, the time-dependent trajectory reveals rapid and secular disk changes in a single two-dimensional representation.

Combining these two uses provides a natural way to connect temporal displacements in the H–C plane with changes in disk properties. For the strongest β Psc excursion, **the nominal disk mass inferred within the adopted VDD model grid decreases by about 0.7 dex, corresponding to a factor of ~ 5, and subsequently returns to approximately its previous level within ~ 370 days. As discussed by Granada et al. (2026c), the mapping between the H–C observables and disk mass explicitly accounts for its dependence on the inferred inclination, although the resulting values remain model dependent and do not represent a full exploration of all degeneracies associated with direct Hα profile fitting.**

If the recovery reflects a genuine increase in disk mass, the observed change corresponds to an average net disk mass-growth rate of order $\sim 4 \times 10^{-9}, M_\odot, {\rm yr}^{-1}$. This quantity should not be identified directly with the stellar mass-injection rate, since the inferred evolution may also contain a geometrical contribution. In particular, the recovery is accompanied by a shift of the preferred models toward larger apparent inclinations, which may reflect changes in the structure or orientation of the Hα-forming region rather than a genuine reorientation of the entire disk.

A dedicated time-dependent model of β Psc, allowing for changes in disk density structure, radial extent, and geometry, will be required to determine how much of the inferred evolution arises from true changes in disk mass and how much results from changes in the line-emitting geometry.

Acknowledgements

We acknowledge the use of spectra from the Be Star Spectra (BeSS) database, maintained at LESIA, Observatoire de Paris. AG and YRC acknowledge support from European Union project 101183150–OCEANS. AG acknowledges project UNRN 40-B-1186. YRC acknowledges UNLP Programa de Incentivos 11/G192.

References

Catalán, R. G., Garay, J., & López-Ruiz, R. 2002, Phys. Rev. E, 66, 011102.

Ghoreyshi, M. R., Jones, C. E., & Granada, A. 2023, "Angular momentum loss rates in Be stars determined by the viscous decretion disc model", MNRAS, 518, 30, doi:10.1093/mnras/stac3084.

Granada, A., Plastino, A. R., & Cochetti, Y. R. 2026a, "Morphology of Emission Spectral Lines in Be Stars: The Entropy–Complexity Plane Approach", J. Phys.: Conf. Ser., 3248, 012001, doi:10.1088/1742-6596/3248/1/012001.

Granada, A., Plastino, A. R., & Cochetti, Y. R. 2026b, "Inclinación en estrellas Be tardías a partir de perfiles Hα: entropía y complejidad", Bol. Asoc. Argent. Astron., 67, 264–267.

Granada, A., Plastino, A. R., Cochetti, Y. R., et al. 2026c, "The entropy–complexity plane as a tracer of Be-star disk dynamics: Application to β Psc", Astron. Astrophys., 713, A30.

Lailey, S., & Sigut, T. A. A. 2023, MNRAS, 527, 2585.

Levenhagen, R. S., Diaz, M. P., Amôres, E. B., & Leister, N. V. 2021, MNRAS, 501, 747.

Neiner, C., de Batz, B., Cochard, F., et al. 2011, AJ, 142, 5, 149.

Rivinius, T., Carciofi, A. C., & Martayan, C. 2013, Astron. Astrophys. Rev., 21, 69.

Vieira, R. G., Carciofi, A. C., Bjorkman, J. E., et al. 2017, MNRAS, 464, 3071.